Robust math xmlns="http://www.w3.org/1998/Math/MathML" display="inline">mrow>mi>d/mi>/mrow>/math>-Wave Superconductivity in the Square-Lattice math xmlns="http://www.w3.org/1998/Math/MathML" display="inline">mrow>mi>t/mi>mtext>−/mtext>mi>J/mi>/mrow>/math> Model

Shoushu Gong, W. Zhu, and D. N. Sheng

Phys. Rev. Lett. **127**, 097003 — Published 27 August 2021

DOI: 10.1103/PhysRevLett.127.097003

Robust d-wave superconductivity in the square-lattice t-J model

Shoushu Gong[1],* W. Zhu[2],† and D. N. Sheng[3]‡
[1]*Department of Physics, Beihang University, Beijing 100191, China*
[2] *School of Science, Westlake University, Hangzhou 310024, China, and*
Institute of Natural Sciences, Westlake Institute of Advanced Study, Hangzhou 310024, China, and
Key Laboratory for Quantum Materials of Zhejiang Province, Westlake University, Hangzhou 310024, China
[3]*Department of Physics and Astronomy, California State University Northridge, California 91330, USA*

Unravelling competing orders emergent in doped Mott insulators and their interplay with unconventional superconductivity is one of the major challenges in condensed matter physics. To explore possible superconducting state in doped Mott insulator, we study the square-lattice t-J model with both the nearest-neighbor and next-nearest-neighbor electron hoppings and spin interactions. By using the state-of-the-art density matrix renormalization group calculation with imposing charge $U(1)$ and spin $SU(2)$ symmetries on the large-scale six-leg cylinders, we establish a quantum phase diagram including three phases: a stripe charge density wave phase, a superconducting phase without static charge order, and a superconducting phase coexistent with a weak charge stripe order. Crucially, we demonstrate that the superconducting phase has a power-law pairing correlation decaying much slower than the charge density and spin correlations, which is a quasi-1D descendant of the uniform d-wave superconductor in two dimensions. These findings reveal that enhanced charge and spin fluctuations with optimal doping is able to produce robust d-wave superconductivity in doped Mott insulators, providing a foundation for connecting theories of superconductivity to models of strongly correlated systems.

Introduction.— To understand the emergence of unconventional superconductivity (SC) is one of the major challenges of modern physics [1, 2]. Despite intensive studies in the past 30 years, it remains elusive if a robust SC state can emerge in the electron systems with strong repulsive interaction. Since the SC phase is usually realized by doping the parent antiferromagnetic compounds such as cuprate-based materials, the Hubbard model and the closely related t-J model are taken as canonical models for studying SC in strongly correlated systems [1–5]. Lacking of well controlled analytical solutions in two dimensions (2D), unbiased computational studies play an important role in establishing the quantum phases in such models. So far, the common consensus is that charge and spin intertwined orders are dominant in lightly doped Hubbard and t-J models on the square lattice, while SC correlations are relatively weak on wider systems [6–19]. The inconsistency of these results with the insight from experimental observations, i.e. a SC "dome" throughout a range of doping parent antiferromagnetic compounds, poses a fundamental challenge to our understanding of strongly correlated electron systems [1, 2].

Intuitively, introducing the next-nearest-neighbor hopping t_2 to the basic Hubbard or t-J models should be more realistic for describing materials [20–22], which may help to weaken charge order and enhance SC [7, 17, 23–27]. Specifically, recent studies of the t_1-t_2 Hubbard model on the width-4 cylinder observed a quasi-long-range SC correlation [28–30], which coexists with the power-law charge density correlation in the form of the Luther-Emery liquid [31–35]. However, a more recent numerical study suggested that there can be different d-wave symmetries in such a system, and a plaquette d-wave correlation may be favored on the width-4 cylinder, which does not represent a true d-wave SC order in the 2D limit [36]. This work also highlights the importance of going to wider systems, which is an essential step towards understanding the competing orders in the 2D limit.

To make a significant progress towards understanding SC in 2D strongly correlated systems, we study the quantum phases in lightly doped square-lattice t-J model using the state-of-the-art density matrix renormalization group (DMRG) [37, 38], and demonstrate a global phase diagram on the width-6 cylinder by tuning doping level δ and hopping ratio t_2/t_1. We identify three distinct phases: a stripe charge density wave (CDW) phase, a uniform d-wave SC phase, and a SC phase coexistent with a weak CDW order. The intermediate uniform SC phase occupies a large portion of the phase diagram upon increasing doping level. The SC correlation has a power-law quasi-long-range order with the Luttinger exponent reaching a small value $K_{sc} \approx 0.36$ and the ordinary d-wave symmetry, which dominates over other correlations. Crucially, through a rigorous bond-dimension scaling, we provide compelling evidence that the SC phase is the quasi-1D descendant of a robust 2D superconductor. These results offer strong evidence that SC order can overtake the tendency of other orderings in a doped Mott insulator, based on which we discuss some insight for doping-induced quantum phase transitions and compare with experimental observations in the cuprate systems.

Solving the t-J model with DMRG.— The extended t-J model is defined as

$$H = -\sum_{\{ij\},\sigma} t_{ij}(\hat{c}^{\dagger}_{i,\sigma}\hat{c}_{j,\sigma} + h.c.) + \sum_{\{ij\}} J_{ij}(\hat{\mathbf{S}}_i \cdot \hat{\mathbf{S}}_j - \frac{1}{4}\hat{n}_i\hat{n}_j),$$

where $\hat{c}^{\dagger}_{i,\sigma}$ and $\hat{c}_{i,\sigma}$ are the creation and annihilation operators for the electron with spin σ ($\sigma = \pm 1/2$) at the site i, $\hat{\mathbf{S}}_i$ is the spin-1/2 operator, and $\hat{n}_i \equiv \sum_\sigma \hat{c}^{\dagger}_{i,\sigma}\hat{c}_{i,\sigma}$ is the electron number operator. We consider the nearest-neighbor (NN) and next-nearest-neighbor (NNN) hoppings (t_1 and t_2) and interactions (J_1 and J_2), as shown in Fig. 1(a). We choose $t_1/J_1 = 3.0$, $J_2/J_1 = (t_2/t_1)^2$ [30] and focus on the region with $0 \leq t_2/t_1 \leq 0.32$ and hole doping level $1/24 \leq \delta \leq 1/6$ which is the optimal region for the SC in the cuprates [20–22].

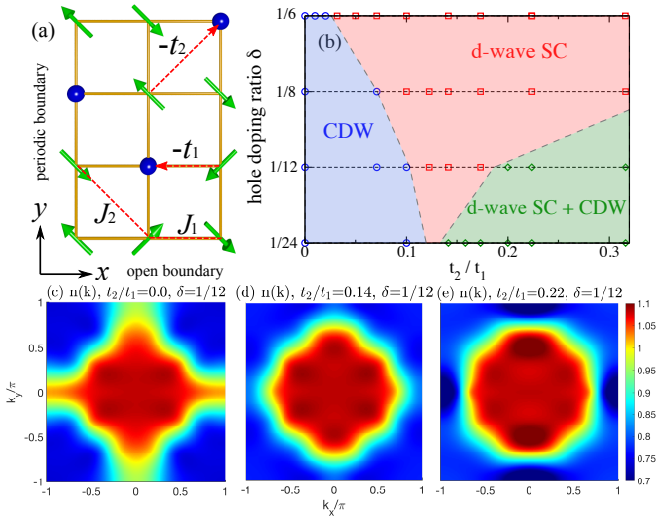

FIG. 1. Global quantum phase diagram. (a) Schematic plot of the t-J model on the square lattice, where arrows and circles respectively denote electrons and doped holes. The model has both the nearest-neighbor and the next-nearest-neighbor hoppings (t_1 and t_2) and spin exchange (J_1 and J_2) interactions. (b) Quantum phase diagram of the model obtained on the $L_y = 6$ cylinder based on the static charge density pattern shown in Fig. 2. For $0 \leq t_2/t_1 \leq 0.32$ and doping level $1/24 \leq \delta \leq 1/6$, we identify a CDW phase, a uniform d-wave SC phase, and a coexistent d-wave SC and CDW (SC + CDW) phase. The Luttinger exponents of SC pairing and density correlations cross over between different phases. Momentum distribution functions $n(\mathbf{k})$ for (c) CDW phase, (d) uniform SC phase, and (e) SC + CDW coexistent phase.

By advancing the DMRG simulations with $U(1) \times SU(2)$ symmetries [39] (also see Supple. Mat. [40]), we study the system on a cylinder with the periodic boundary conditions along the circumference direction (y) and the open boundary along the axis direction (x), where L_y and L_x denote the lattice sites along these two directions. We keep the bond dimensions up to $D = 20000$ $SU(2)$ multiplets, which is equivalent to about 60000 $U(1)$ states (it is about double of the previous standard in the literatures for the t-J model [18, 30]) and thus allows us to obtain accurate results on the $L_y = 6$ cylinder with the truncation error near 1×10^{-6} [40].

Quantum phase diagram.— Figure 1 presents the phase diagram as a function of t_2/t_1 and doping level δ based on comprehensive simulations of cylinder systems with $L_x = 48, 64$ and $L_y = 6$. We identify three phases with different charge density distributions: a CDW phase (light purple), a d-wave SC phase without static charge order (red), and a SC + CDW coexistent phase (green). In the CDW phase, we identify stripe orders with wavelength $\lambda \simeq 4/(L_y\delta)$ depending on doping level (Fig. 2(a)), consistent with previous results [13, 16, 17]. Meanwhile, SC pairing correlations are weak and become very small at long distance near $t_2 = 0$ (Fig. 3(b)). In the SC phase, we find uniform charge density without static charge order (Fig. 2(b)), but with a strong quasi-long-range SC order of the ordinary d-wave symmetry (Fig. 3(a)). For the coexistent phase, we also find a dominant quasi-long-range SC order (Fig. 3(b)), which cooperates with a weak stripe order with wavelength $\lambda \simeq 2/(L_y\delta)$ (Fig. 2(c)).

The intermediate uniform SC phase is the key finding in this paper. Interestingly, the window of the d-wave SC phase gradually spans with increasing doping level, inducing the doping-tuned CDW (or SC + CDW coexistent phase) to a uniform SC phase transition. As we will discuss below, this picture could be relevant to experimental observations in cuprates. In the following, we turn to the identification of these phases.

Charge density wave.— Since the charge density of the ground state is uniform along the y direction due to translational symmetry and shows distinct behaviors along the x direction for different phases, we define the averaged charge density for each column as $n_x = \sum_{y=1}^{L_y} \langle \hat{n}_{x,y} \rangle / L_y$ and show the density profiles in Fig. 2. In the CDW phase, we identify an approximate periodic density modulation with the wavelength $\lambda \simeq 4/(L_y\delta)$ doping dependent. For example, at $t_2 = 0, \delta = 1/12$, the density profile has $\lambda \simeq 8$, i.e. each stripe is filled with four holes (or $n^h_{str} = 4$ in average, see Fig. 2(a)). In contrast, in the coexistent phase we find a charge modulation with $\lambda \simeq 4$ (Fig. 2(c)), which contains two holes $n^h_{str} = 2$ in average per stripe, regardless of the doping level. Thus, a quasi-long-range SC occurs likely in the coexistent phase as the charge modulation with two holes ($n^h_{str} = 2$) may be plausible for pairing [30, 41–43]. Importantly, in addition to the aforementioned charge ordered phases, we find a uniform charge density phase with vanishing-small density

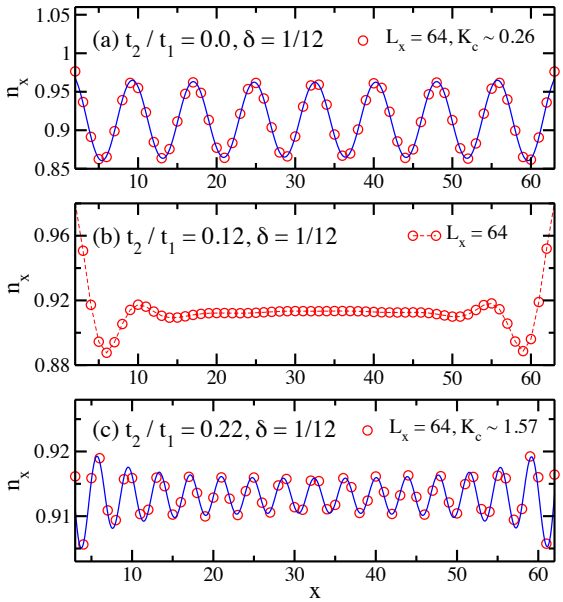

FIG. 2. Charge density profiles. The charge density distributions $n_x = \sum_{y=1}^{L_y} \langle \hat{n}_{x,y} \rangle / L_y$ on the $L_x = 64, L_y = 6$ cylinder for (a) CDW phase, (b) SC phase, and (c) SC + CDW phase. The blue lines are fitting curves to the function $n_x = n_0 + A_{cdw} \cos(Qx + \phi)$, where $A_{cdw} = A_0(x^{-K_c/2} + (L_x + 1 - x)^{-K_c/2})$ and Q are the CDW amplitude and wave vector, respectively. ϕ is a phase shift.

modulation in the bulk of system (see Fig. 2(b)) and [40]). The absence of static charge order indicates that CDW is very weak and thus may give the way to a robust SC.

SC pairing correlation and d-wave symmetry.— We examine the SC by measuring the dominant spin-singlet pairing correlations $P_{\alpha,\beta}(\mathbf{r}) = \langle \hat{\Delta}^{\dagger}_{\alpha}(\mathbf{r}_0)\hat{\Delta}_{\beta}(\mathbf{r}_0+\mathbf{r})\rangle$, where the pairing operator is defined on two NN sites $\mathbf{r}_1$ and $\mathbf{r}_2 = \mathbf{r}_1 + \mathbf{e}_\alpha$ and $\hat{\Delta}_\alpha(\mathbf{r}_1) = (c_{\mathbf{r}_1\uparrow}c_{\mathbf{r}_2\downarrow} - c_{\mathbf{r}_1\downarrow}c_{\mathbf{r}_2\uparrow})/\sqrt{2}$ ($\mathbf{e}_{\alpha=x,y}$ denote the unit lengths along x- and y-direction, respectively). We consider correlation decay along the x direction with distance r.

First, we discuss the SC pairing symmetry by inspecting the different pairing correlations shown in Fig. 3(a). While two kinds of the vertical-vertical correlations $P_{y,y}$ (blue, for two y-bonds in the same chains), $P''_{y,y}$ (red, for two y-bonds with one relative lattice shift in the y-direction) and the horizontal-horizontal correlation $P_{x,x}$ (purple) are always positive, the vertical-horizontal correlations $P_{y,x}$ (green) are negative. Thus, the pairing order parameters should have the opposite signs for the x-bond and y-bond, respectively. Furthermore, the pairing term has no phase shift along both directions, showing a conventional d-wave pairing symmetry as depicted by the inset of Fig. 3(a). In addition, the magnitudes of the pairing correlations are insensitive to bond orientations, showing a spatially uniform feature of the SC order. Second, by tuning t_2/t_1, the pairing correlations are enhanced and become strong in the SC phase, signaling the developed quasi-long-range order. Such pairing correlations remain stable for the larger t_2/t_1 entering the SC + CDW phase as shown in Fig. 3(b) for $\delta = 1/12$. Third, in the SC and SC + CDW phases, we identify that the pairing correlation dominates over all other competing charge and spin correlations, as evidenced by Fig. 5 for $\delta = 1/12, t_2/t_1 = 0.12$ (SC phase) and 0.22 (SC + CDW phase). All above features strongly support a robust d-wave pairing nature in the SC and the SC + CDW phases.

To clarify the presence of quasi-long-range SC order, we further investigate the decay behavior of pairing correlations using two different ways. As DMRG method represents the ground state as a Matrix product state with a finite bond dimension, the correlations at long distance usually decay exponentially on wider systems [44], which would recover the true nature of correlations in the infinite bond dimension limit. Therefore, we first fit the raw data of pairing correlations for various bond dimensions using the exponential function $P_{y,y}(r) \sim \exp(-r/\xi_{sc})$, as shown in Fig. 4(a). One can see that the correlation length ξ_{sc} monotonically grows as the bond dimension increases. We find a power-law dependence $\xi_{sc} \sim D^{\alpha}$ (see the inset of Fig. 4(a)) for the bond dimension up to $D = 20000$, indicating that ξ_{sc} tends to diverge in the $D \to \infty$ limit and a true quasi-long-range order is expected. In the second method, the obtained SC correlations are extrapolated to the $D \to \infty$ limit first [19, 29], using a second-order polynomial function of $1/D$ for the data points of $D = 8000 - 20000$ (Fig. 4(b)). We find that the extrapolated pairing correlations over a wide range of distance collapse to a power-law decay function $P_{y,y}(r) \sim r^{-K_{sc}}$, with a Luttinger exponent $K_{sc} \approx 0.36$. In Fig. 4(c), we compare the power-law SC correlations on the $L_y = 4$ and 6 systems, which give the exponent $K_{sc} \approx 0.96$ for $L_y = 4$ and 0.36 for $L_y = 6$. It is clear that the pairing correlations are significantly enhanced for $L_y = 6$ and we find that $K_{sc} < 1$ is a common feature in the SC phase [40]. It signals that the SC order, which becomes stronger and tends to be stabilized on

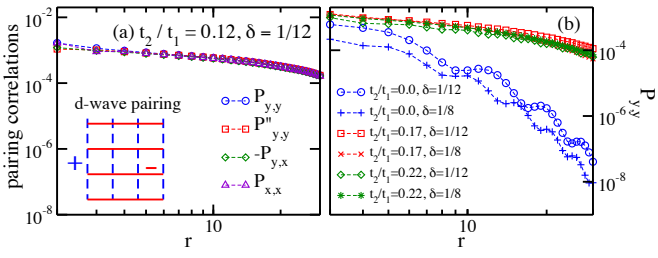

FIG. 3. SC pairing correlations. (a) Various kinds of pairing correlations along different bond directions: vertical-vertical correlation $P_{y,y}$ (blue) and $P''_{y,y}$ (red), horizontal-horizontal correlation $P_{x,x}$ (purple), and vertical-horizontal correlation $P_{y,x}$ (green). The inset shows the pattern of the d-wave symmetry. (b) Double-logarithmic plot of the pairing correlations $P_{y,y}$ for different t_2/t_1 at $\delta = 1/12, 1/8$.

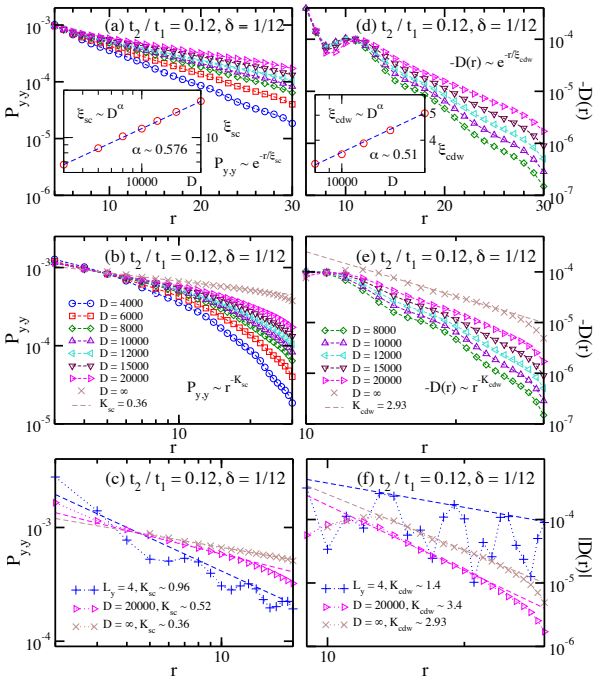

FIG. 4. Scaling of correlations in the SC phase. (a) Semi-logarithmic plot of $P_{y,y}$ obtained by different bond dimensions D. The inset shows the dependence of the correlation length ξ_{sc} on D, where ξ_{sc} is obtained by fitting $P_{y,y} \sim \exp(-r/\xi_{sc})$. In the range of $D = 4000 - 20000$ (equivalent to $U(1)$ $D = 12000 - 60000$), ξ_{sc} fits to $\xi_{sc} \sim D^{\alpha}$ with $\alpha = 0.576$. (b) Double-logarithmic plot of $P_{y,y}$ with the same data in the subfigure (a). The dashed crossed line denotes the power-law fitting of the extrapolated $D \to \infty$ results. (c) Comparing the pairing correlations on the $L_y = 4, 6$ cylinders. (d-f) Similar plots for the density-density correlation function $D(r)$.

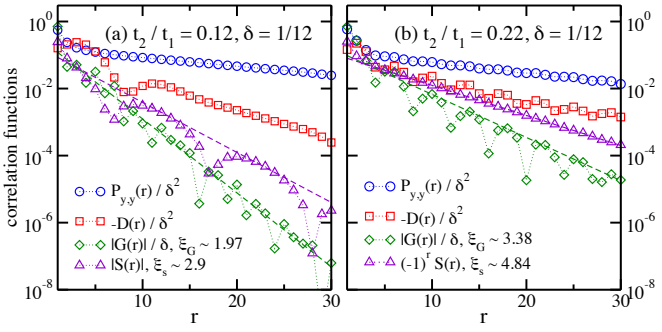

FIG. 5. Correlations in the SC and SC + CDW phases. Comparison among the pairing correlation $P_{y,y}(r)$, density correlation $D(r)$, spin correlation $S(r) = \langle \mathbf{S}_x \cdot \mathbf{S}_{x+r} \rangle$, and single particle correlation $G(r) = \langle \sum_\sigma c^\dagger_{x,\sigma} c_{x+r,\sigma} \rangle$ for (a) SC phase and (b) SC + CDW phase. The correlations are rescaled to make a direct comparison.

larger system sizes, should survive in the 2D limit. Thus, this uniform SC state can be regarded as the quasi-1D descendant of a 2D superconductor [32].

Last but not least, we compare density correlations with SC pairing correlations. We identify a power-law behavior of density correlations with a much higher exponent $K_{cdw} \approx 2.93$ (see Fig. 4(d,e)). In Fig. 4(c,f) we show that SC pairing and density correlations behave differently going from width-4 to width-6 cylinder: while SC correlations greatly enhance (K_{sc} reduces from 0.96 to 0.36), density correlations are strongly suppressed with K_{cdw} increasing from 1.4 to 2.93. Notice that $K_{sc} < 0.5$ and $K_{cdw} > 2$ imply that the SC susceptibility diverges whereas the CDW susceptibility remains finite on the ladder systems [33]. This trend indicates that the SC order may grow stronger with increasing system width, thus we anticipate a robust uniform SC phase without a CDW instability in the 2D limit. Furthermore, we have carefully confirmed that the single-particle and spin correlations all decay exponentially in the uniform SC phase (see Fig. 5(a) and [40]).

In comparison, in the SC + CDW phase the SC order is found to cooperate with a weak stripe order, qualitatively consistent with the results of the width-4 Hubbard model or t-J model [29, 30]. Quantitatively, SC correlations still dominate all other correlations (see Fig. 5(b)) with the Luttinger exponents $K_{sc} < K_{cdw} < 2$ (see Supple. Mat. [40]).

Fermi surface evolution.— Lastly we measure the electron distribution function in the momentum space $n(\mathbf{k}) = \sum_{i,j,\sigma} \langle c^\dagger_{i,\sigma} c_{j,\sigma} \rangle e^{i\mathbf{k}\cdot(\mathbf{r}_i - \mathbf{r}_j)}/(L_x L_y)$ to study the evolution of electronic structure. We identify that the normal and SC phases have distinct topologies of $n(\mathbf{k})$: In the normal CDW phase (Fig. 1(c)), the size of the electron pocket near the $\Gamma = (0, 0)$ point expands eventually covering a large portion of the Brillouin zone with a clear nematic distortion of Fermi surface from the unidirectional stripe order. In the SC and SC + CDW phases (Fig. 1(d-e)), electronic states form a closed Fermi surface with approximate C_4 symmetry and an isolated electron pocket centers around the Γ point. Such a change of the Fermi surface topology is robust for all doping levels [40]. We conjecture that the Fermi surface topology may be related to the emergence of quantum criticality between the CDW and SC phase, which we leave for future study.

Summary and Discussion.— We have presented a comprehensive study of a doped Mott insulator by further advancing the state-of-the-art DMRG computations, which allows us to identify a robust superconductivity on wider cylindrical systems. We map out a global phase diagram in terms of doping level and the NNN electron hopping strength. We identify two SC phases, either with or without a static CDW order. The remarkable result found on the wider system is that, by suppressing charge and spin orders, a uniform SC phase with the ordinary d-wave pairing symmetry emerges. We carefully established that the SC pairing correlation is the strongest correlation with robust quasi-long-range order and a small power exponent. The density correlations also decay with a power-law behavior, but has a large exponent, indicating a special limit of Luther-Emery liquid where the CDW correlations cannot compete with the SC correlations. Such a uniform d-wave SC state has been sought for decades, and the current numerical identification provides convincing evidence for the emergent of such a state in strongly correlated electron systems with only repulsive interactions.

As the width-6 system has reduced ring and plaquette correlations around the cylinder [36], it may be a better representation of 2D system. Intuitively, our phase diagram on the 6-leg system turns out to resemble the essential features of the cuprate compounds [2]. For instance, upon increasing the hole doping level, two different possibilities could occur: the system could be driven from the normal state to a uniform SC phase directly, or it could first go into a SC + CDW coexistent phase and then it takes another transition into a uniform SC state. This picture provides an intuitive understanding that CDW order often but not always appears in the underdoped regime with the onset of superconductivity, which may depend on the ratio t_2/t_1 and other properties of materials.

Acknowledgments.— We acknowledge stimulating discussions with L. Balents, H. C. Jiang, S.A. Kivelson and R. H. He. This work was supported by the NSFC grants 11834014, 11874078, and the Fundamental Research Funds for the Central Universities (S.S.G.). W.Z. was supported by the foundation of Westlake University. This work was also supported by the U.S. Department of Energy, Office of Science, Advanced Scientific Computing Research and Basic Energy Sciences, Materials Sciences and Engineering Division, Scientific Discovery through Advanced Computing (SciDAC) program under the grant number DE-AC02-76SF00515 (D.N.S.).

Note added.— At the final stage of preparing this work, we notice an arXiv preprint focusing on larger positive t_2 regime [45] and another preprint studying the phase diagram with both negative and positive t_2 [46]. The superconducting state found in Ref. [45] has the similar pairing correlation and density correlation power exponents as those in our SC + CDW state. The enhanced spin correlations with growing system circumference in the SC + CDW phase also agree with the observation in Ref. [46] in the same parameter region.

* shoushu.gong@buaa.edu.cn
† zhuwei@westlake.edu.cn
‡ donna.sheng1@csun.edu

[1] B. Keimer, S. A. Kivelson, M. R. Norman, U. S., and J. Zaanen, Nature **518**, 179 (2015), URL https://doi.org/10.1038/nature14165.

[2] C. Proust and L. Taillefer, Annual Review of Condensed Matter Physics **10**, 409 (2019), URL https://doi.org/10.1146/annurev-conmatphys-031218-013210.

[3] P. A. Lee, N. Nagaosa, and X.-G. Wen, Rev. Mod. Phys. **78**, 17 (2006), URL https://link.aps.org/doi/10.1103/RevModPhys.78.17.

[4] M. Ogata1 and H. Fukuyama, Rep. Porg. Phys. **71**, 036501 (2008), URL https://iopscience.iop.org/article/10.1088/0034-4885/71/3/036501.

[5] Z. Y. Weng, D. N. Sheng, Y.-C. Chen, and C. S. Ting, Phys. Rev. B **55**, 3894 (1997), URL https://link.aps.org/doi/10.1103/PhysRevB.55.3894.

[6] S. R. White and D. J. Scalapino, Phys. Rev. Lett. **80**, 1272 (1998), URL https://link.aps.org/doi/10.1103/PhysRevLett.80.1272.

[7] S. R. White and D. J. Scalapino, Phys. Rev. B **60**, R753 (1999), URL https://link.aps.org/doi/10.1103/PhysRevB.60.R753.

[8] S. R. White and D. J. Scalapino, Phys. Rev. Lett. **91**, 136403 (2003), URL https://link.aps.org/doi/10.1103/PhysRevLett.91.136403.

[9] S. Sorella, G. B. Martins, F. Becca, C. Gazza, L. Capriotti, A. Parola, and E. Dagotto, Phys. Rev. Lett. **88**, 117002 (2002), URL https://link.aps.org/doi/10.1103/PhysRevLett.88.117002.

[10] G. Hager, G. Wellein, E. Jeckelmann, and H. Fehske, Phys. Rev. B **71**, 075108 (2005), URL https://link.aps.org/doi/10.1103/PhysRevB.71.075108.

[11] P. Corboz, T. M. Rice, and M. Troyer, Phys. Rev. Lett. **113**, 046402 (2014), URL https://link.aps.org/doi/10.1103/PhysRevLett.113.046402.

[12] J. P. F. LeBlanc, A. E. Antipov, F. Becca, I. W. Bulik, G. K.-L. Chan, C.-M. Chung, Y. Deng, M. Ferrero, T. M. Henderson, C. A. Jiménez-Hoyos, et al. (Simons Collaboration on the Many-Electron Problem), Phys. Rev. X **5**, 041041 (2015), URL https://link.aps.org/doi/10.1103/PhysRevX.5.041041.

[13] B.-X. Zheng, C.-M. Chung, P. Corboz, G. Ehlers, M.-P. Qin, R. M. Noack, H. Shi, S. R. White, S. Zhang, and G. K.-L. Chan, Science **358**, 1155 (2017), ISSN 0036-8075, URL https://science.sciencemag.org/content/358/6367/1155.

[14] G. Ehlers, S. R. White, and R. M. Noack, Phys. Rev. B **95**, 125125 (2017), URL https://link.aps.org/doi/10.1103/PhysRevB.95.125125.

[15] E. W. Huang, C. B. Mendl, S. Liu, S. Johnston, H.-C. Jiang, B. Moritz, and T. P. Devereaux, Science **358**, 1161 (2017), URL https://science.sciencemag.org/content/358/6367/1161.

[16] K. Ido, T. Ohgoe, and M. Imada, Phys. Rev. B **97**, 045138 (2018), URL https://link.aps.org/doi/10.1103/PhysRevB.97.045138.

[17] B. Ponsioen, S. S. Chung, and P. Corboz, Phys. Rev. B **100**, 195141 (2019), URL https://link.aps.org/doi/10.1103/PhysRevB.100.195141.

[18] H.-C. Jiang, Z.-Y. Weng, and S. A. Kivelson, Phys. Rev. B **98**, 140505 (2018), URL https://link.aps.org/doi/10.1103/PhysRevB.98.140505.

[19] M. Qin, C.-M. Chung, H. Shi, E. Vitali, C. Hubig, U. Schollwöck, S. R. White, and S. Zhang (Simons Collaboration on the Many-Electron Problem), Phys. Rev. X **10**, 031016 (2020), URL https://link.aps.org/doi/10.1103/PhysRevX.10.031016.

[20] E. Pavarini, I. Dasgupta, T. Saha-Dasgupta, O. Jepsen, and O. K. Andersen, Phys. Rev. Lett. **87**, 047003 (2001), URL https://link.aps.org/doi/10.1103/PhysRevLett.87.047003.

[21] K. Tanaka, T. Yoshida, A. Fujimori, D. H. Lu, Z.-X. Shen, X.-J. Zhou, H. Eisaki, Z. Hussain, S. Uchida, Y. Aiura, et al., Phys. Rev. B **70**, 092503 (2004), URL https://link.aps.org/doi/10.1103/PhysRevB.70.092503.

[22] C. Kim, P. J. White, Z.-X. Shen, T. Tohyama, Y. Shibata, S. Maekawa, B. O. Wells, Y. J. Kim, R. J. Birgeneau, and M. A. Kastner, Phys. Rev. Lett. **80**, 4245 (1998), URL https://link.aps.org/doi/10.1103/PhysRevLett.80.4245.

[23] S. R. White and D. J. Scalapino, Phys. Rev. B **79**, 220504 (2009), URL https://link.aps.org/doi/10.1103/PhysRevB.79.220504.

[24] C. T. Shih, T. K. Lee, R. Eder, C.-Y. Mou, and Y. C. Chen, Phys. Rev. Lett. **92**, 227002 (2004), URL https://link.aps.org/doi/10.1103/PhysRevLett.92.227002.

[25] G. B. Martins, J. C. Xavier, L. Arrachea, and E. Dagotto, Phys. Rev. B **64**, 180513 (2001), URL https://link.aps.org/doi/10.1103/PhysRevB.64.180513.

[26] M. Bejas, A. Greco, and H. Yamase, Phys. Rev. B **86**, 224509 (2012), URL https://link.aps.org/doi/10.1103/PhysRevB.86.224509.

[27] A. Eberlein and W. Metzner, Phys. Rev. B **89**, 035126 (2014), URL https://link.aps.org/doi/10.1103/PhysRevB.89.035126.

[28] J. F. Dodaro, H.-C. Jiang, and S. A. Kivelson, Phys. Rev. B **95**, 155116 (2017), URL https://link.aps.org/doi/10.1103/PhysRevB.95.155116.

[29] H.-C. Jiang and T. P. Devereaux, Science **365**, 1424 (2019), ISSN 0036-8075, URL https://science.sciencemag.org/content/365/6460/1424.

[30] Y.-F. Jiang, J. Zaanen, T. P. Devereaux, and H.-C. Jiang, Phys. Rev. Research **2**, 033073 (2020), URL https://link.aps.org/doi/10.1103/PhysRevResearch.2.033073.

[31] A. Luther and V. J. Emery, Phys. Rev. Lett. **33**, 589 (1974), URL https://link.aps.org/doi/10.1103/PhysRevLett.33.589.

[32] L. Balents and M. P. A. Fisher, Phys. Rev. B **53**, 12133 (1996), URL https://link.aps.org/doi/10.1103/PhysRevB.53.12133.

[33] E. Arrigoni, E. Fradkin, and S. A. Kivelson, Phys. Rev. B **69**, 214519 (2004), URL https://link.aps.org/doi/10.1103/PhysRevB.69.214519.

[34] Y. Gannot, Y.-F. Jiang, and S. A. Kivelson, Phys. Rev. B **102**, 115136 (2020), URL https://link.aps.org/doi/10.1103/PhysRevB.102.115136.

[35] H.-C. Jiang, S. Chen, and Z.-Y. Weng, Phys. Rev. B **102**, 104512 (2020), URL https://link.aps.org/doi/10.1103/PhysRevB.102.104512.

[36] C.-M. Chung, M. Qin, S. Zhang, U. Schollwöck, and S. R. White (The Simons Collaboration on the Many-Electron Problem), Phys. Rev. B **102**, 041106 (2020), URL

https://link.aps.org/doi/10.1103/PhysRevB.102.041106.
[37] S. R. White, Phys. Rev. Lett. **69**, 2863 (1992).
[38] S. R. White, Phys. Rev. B **48**, 10345 (1993).
[39] I. P. McCulloch and M. Gulácsi, Europhysics Letters (EPL) **57**, 852 (2002), URL https://doi.org/10.1209%2Fepl%2Fi2002-00393-0.
[40] See Supplemental Material for more supporting data.
[41] J. Zaanen and O. Gunnarsson, Phys. Rev. B **40**, 7391 (1989), URL https://link.aps.org/doi/10.1103/PhysRevB.40.7391.
[42] M. Vojta, Advances in Physics **58**, 699 (2009).
[43] K. Machida, Physica C: Superconductivity **158**, 192 (1989), ISSN 0921-4534.
[44] U. Schollwöck, Annals of Physics **326**, 96 (2011), january 2011 Special Issue, URL http://www.sciencedirect.com/science/article/pii/S0003491610001752.
[45] H.-C. Jiang and S. A. Kivelson, arXiv e-prints arXiv:2104.01485 (2021), 2104.01485.
[46] S. Jiang, D. J. Scalapino, and S. R. White, arXiv e-prints arXiv:2104.10149 (2021), 2104.10149.